ДГКС Друштво грађевинских конструктера Србије
ASES Association of Structural Engineers of Serbia
R-11 Kongres 2022 Congress 2022

Jelena Nikolić[1], *Svetlana M. Kostić*[2], *Saša Stošić*[3]

NUMERIČKO MODELIRANJE AKSIJALNE NOSIVOSTI STUBOVA OD ČELIČNIH CEVI ISPUNJENIH BETONOM

Rezime:

U radu je prikazano numeričko modeliranje aksijalne nosivosti kratkih stubova od čeličnih cevi ispunjenih betonom. Za potrebe analize napravljen je nelinearni 3D model na bazi konačnih elemenata u programu ABAQUS. Modeliranje, granični uslovi, konstitutivni modeli za čelik i beton i interakcija na kontaktu čelične cevi i betona detaljno su razmotreni. Predložena su tri numerička modela koji su validirani pomoću prikupljenih rezultata eksperimenata. Na kraju, aksijalna nosivost spregnutog stuba upoređena je sa nosivošću sračunatom po Evrokodu 4.

Ključne reči: spregnuti stubovi, nelinearna analiza, metod konačnih elemenata

NUMERICAL MODELLING OF CONCRETE-FILLED STEEL TUBE COLUMNS UNDER AXIAL COMPRESSION

Summary:

The paper presents the numerical modelling of concrete-filled steel tube stub columns under axial compression. The nonlinear 3D finite element model for the analysis was developed using ABAQUS software. The modelling, boundary conditions, the constitutive models for steel and concrete and contact interaction between the steel tube and concrete surface are discussed in detail. Three numerical models are proposed and validated using collected experimental data results. Finally, the composite column axial capacity is compared with the Eurocode 4 calculations for composite columns.

Key words: composite columns, nonlinear analysis, finite element analysis

[1] *Asistent, Građevinski fakultet Univerziteta u Beogradu, jnikolic@grf.bg.ac.rs*
[2] *V. prof, Građevinski fakultet Univerziteta u Beogradu, svetlana@grf.bg.ac.rs*
[3] *V. prof, Građevinski fakultet Univerziteta u Beogradu, sasa@grf.bg.ac.rs*

1. INTRODUCTION

A concrete-filled steel tube column (CFST) consists of an outer steel tube filled with concrete. The composite action between two materials provides that the concrete stiffens the steel tube and postpones local buckling. In turn, the outer steel tube acts as longitudinal and transverse reinforcement, permanent formwork and provides confinement for the concrete core. CFST columns demonstrated excellent structural behaviour due to their high strength, ductility, and good seismic behaviour.

Due to their overall good performance, CFST columns have been widely used in different types of construction and are still very present in many research fields [1]. Various shapes and types of CFST columns have been constructed in the past [2-5]. Besides, other materials such as fibre-reinforced concrete or fibre-reinforced polymer sheets (FRP) have been used for strengthening the CFST columns [6-7]. In addition, the global tendency to reuse construction waste as alternative aggregate to produce sustainable concrete resulted in hybrid structural members – recycled aggregate concrete-filled steel tubular (RACFST) columns filled with recycled aggregate concrete [8-10].

The numerical model of CFST columns needs to effectively predict structural members' behaviour and provide complex information regarding their structural response [11]. This paper presents a finite element (FE) model of CFST columns under axial loading in ABAQUS [12]. This analysis method has been widely used in the literature to validate experimental results [1-5]. In addition, the FE model in ABAQUS can predict other important information, such as failure modes and deformation patterns, or capture phenomena such as local buckling of the steel tube and confinement of the concrete [8].

The idea was to develop reliable but a simple model, especially in terms of geometry and test setup simulation, boundary conditions and loading. Analysis was performed as displacement controlled and included both material and geometrical nonlinearities.

3D numerical models presented in this paper are validated with the test results available from the literature and previously developed FE models. Because of page limitations, the validation will be presented by comparison with just two specimens from different studies, 3HN [13] and CC-0 [8]. Finally, the ultimate strength results will be compared to the axial capacity of the cross-section calculated by Eurocode 4 (EC4)[14-15].

2. NUMERICAL MODELLING

2.1. MODEL DESCRIPTION

The outer steel tube and the concrete core were modelled using 8-node brick elements (C3D8R) with three translation degrees of freedom at each node. The mesh size was selected following the mesh convergence studies and recommendations provided in [11]. The finite element mesh across the cross-section was chosen as *D/15* and 2.5 times for the mesh in the longitudinal direction, where *D* refers to the outer diameter of a circular column.

The steel end plates used in tests are not included in the 3D model to simplify the modelling and shorten the calculation time. Instead, the constraints option available in ABAQUS is applied. It connects all surface nodes to only one reference point (RP) defined in the centre of the column's top and bottom surface. As shown in Figure 1, boundary conditions (BC) are set to RP1 and RP2 only: all displacements are restrained except displacement in the loading direction at the RP1. A displacement-controlled axial loading scheme was applied to the RP1 only.

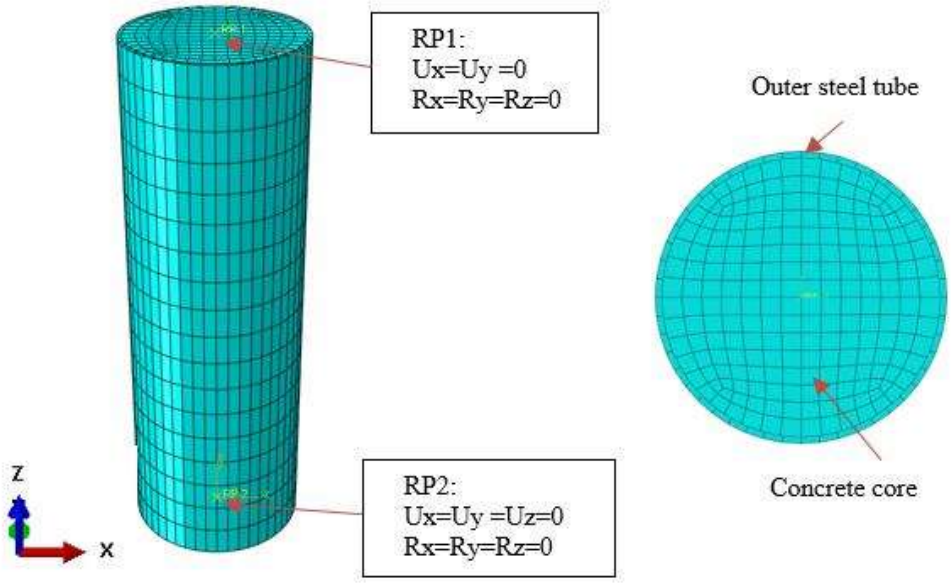

Figure 1 – 3D model of CFST column with RP1 and RP2 with BC; Cross-section and meshing

Interaction between steel tube and concrete core was simulated using the surface-to-surface contact option. The inner tube surface was chosen as the master surface, while the concrete surface was defined as the slave surface. It was essential to allow the separation of the materials in tension and provide no penetration of concrete core into steel tube in compression. The normal behaviour was defined via the "hard" contact option, while tangential behaviour was penalised with a friction coefficient of 0.6, as suggested in [16].

2.2. MATERIAL MODELLING

Numerical modelling of structural steel and concrete constitutive materials followed recommendations by [11] and [16]. This way, two different models were created: Model 1 and Model 2. The third numerical model, denoted as Model 3, investigated material curves proposed by Pre-norm Eurocode 2 (EC2) [17] and Eurocode 3 (EC3) [18] for concrete and steel, respectively. Therefore, three different models have been presented in this paper, as summarized in Table 1.

Table 1 – Numerical models with details of material modelling

	Structural steel	Concrete
Model 1	Tao et al. [11]	Tao et al. [11]
Model 2	Han et al. [16]	Han et al. [16]
Model 3	EC3 [18]	EC2 [17] extended

2.2.1. Material modelling of steel tube

Structural steel properties required for ABAQUS are provided within a uniaxial stress-strain relationship σ-ε. Key input parameres for defining the curve are yield strength f_y, modulus of elasticity E, and the plasticity parameters depending on the chosen curve.

Researchers have investigated stress-strain constitutive models for carbon steel, such as elastic-perfectly plastic, bilinear, and multilinear with hardening [4, 7].

In this paper, three different constitutive models have been considered as illustrated in Figure 2 for specimen 3HN. The first stress-strain curve is proposed in [11] and consists of an elastic branch until the yield strain ε_y, a perfectly plastic branch until $15\varepsilon_y$ and hardening until the ultimate strain ε_u. Hardening is defined by strain-hardening exponent p.

The second is the five-stage elastic-plastic stress-strain model presented in [16]. It consists of elastic, elastic-plastic, plastic, hardening and fracture defined with $\varepsilon_e=0.8f_y/E$, $\varepsilon_{e1}=1.5\varepsilon_e$, $\varepsilon_{e2}=10\varepsilon_{e1}$, $\varepsilon_{e3}=100\varepsilon_{e1}$ respectively, where ε_e is the yield strain and E modulus of elasticity.

The third constitutive model presented is an elastic-perfectly plastic σ-ε relationship for structural steel given in EC3. Material properties for steel used in tests 3HN and CC-0 are provided in Table 2. Poisson's ratio is taken as 0.3.

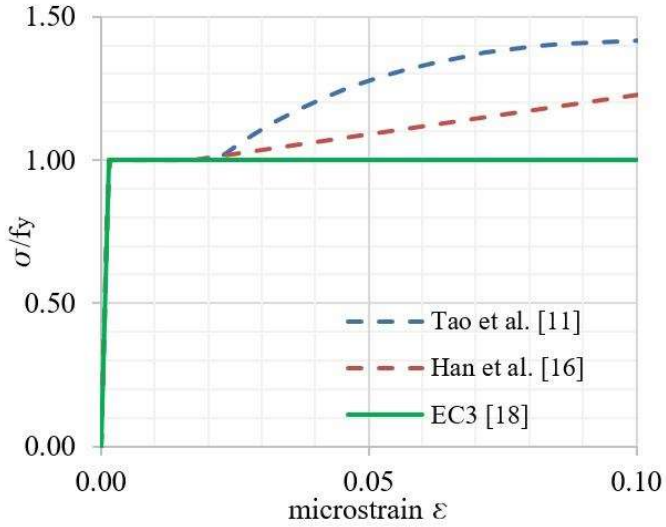

Figure 2 – Constitutive models for the steel tube demonstrated on specimen 3HN [13]

However, this study showed that the choice of the steel stress-strain model did not significantly impact the numerical results. The same observation was previously reported in the literature [4].

2.2.2. Material modelling of concrete core

When the CFST column is subjected to axial compression, concrete reaches a triaxial stress state due to passive confinement provided by the steel tube [11]. This confinement effect is more significant in circular than square columns, as reported in [19].

The concrete Damaged Plasticity (CDP) formulation available in ABAQUS was used to define the nonlinear behaviour of the concrete. Besides, the compressive stress-strain curve of unconfined concrete can be directly defined as the input for the CDP model. However, the model

should include concrete confinement, especially in circular CFST columns. Modelling confined concrete behaviour in CFST columns has been very challenging for many authors. The researchers proved that the passive confinement would increase both the peak strain (ductility) and the strength of the concrete and so the CFST column. One of the possibilities to include the confinement effect in ABAQUS is by modifying the concrete stress-strain curve. This means including softening and hardening behaviour as a result of composite action during the lateral expansion of concrete. This paper has considered three uniaxial models illustrated in Figure 3 for specimen 3HN.

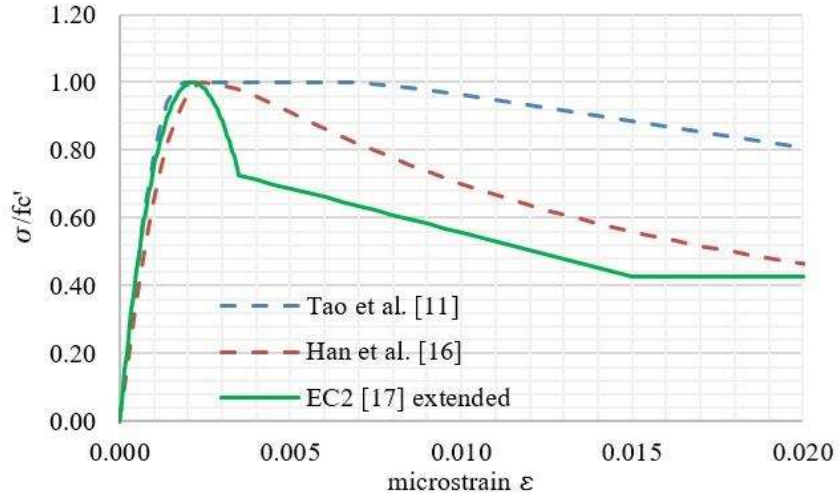

Figure 3 – Constitutive models for the concrete core for specimen 3HN [13]

The first model by Tao et al. suggested that a concrete σ-ε relation considers strain hardening/softening function for confined concrete as the increase in plastic strain (ductility) [11]. The second model by Han et al. is well known for giving good predictions in CDP model in ABAQUS [16]. It defines concrete plastic behaviour depending on the confinement factor ξ. The third model considered is the EC2 stress-strain relation for unconfined concrete in compression with a total strain limit of 3.5‰ [17]. The ascending branch is taken linear elactic until $0.4f_{c'}$ and nonlinear in the plastic region defined by expressions given in Pre-norm EC2 [17]. Beyond strain limit of 3.5‰ , the curve is extended partly following the recommendations for numerical modelling of CFST columns provided in [20]. The residual stress σ_{res} depends on the D/t ratio and concrete compressive strength $f_{c'}$ as given in expression (1). This stress value σ_{res} is reached at the strain of 15‰ and remains constant until the strain of 20‰. For creating Model 3, a simple solution is suggested for defining the stress-strain curve in range 3.5-15‰, with a linear stress-strain branch.

$$\boldsymbol{\sigma_{res}} = \begin{Bmatrix} \mathbf{f_c} & \frac{\mathbf{D}}{\mathbf{t}} \leq \mathbf{24} \\ \mathbf{f_c}\left(\mathbf{1.6 - 0.025}\frac{\mathbf{D}}{\mathbf{t}}\right) & \mathbf{24} < \frac{\mathbf{D}}{\mathbf{t}} \leq \mathbf{64} \\ \mathbf{0} & \mathbf{64} < \frac{\mathbf{D}}{\mathbf{t}} \end{Bmatrix} \quad (1)$$

Furthermore, for application of CDP model several parameters define concrete plasticity: dilation angle *(ψ)*, flow potential eccentricity *(e)*, a ratio of the compressive strength under biaxial loading to uniaxial compressive strength *(f_{b0}/f_c'),* the ratio of the second stress invariant on the tensile meridian to that on the compressive meridian *(K_c)* and viscosity parameter. These parameters have been selected as per Tao et al. for Model 1, while Models 2 and 3 have same values as recommended by and Han et al.: 30º, 0.1, 1.16, 2/3 and 0 correspondingly.

Concrete tensile behaviour in the ABAQUS CDP model for Models 1 and 2 was defined following the same recommendations as in their compressive models. Since EC2 does not provide a curve for concrete in tension, Model 3 has the same tension characteristics adopted for Model 2. Damage parameters are not included in modelling as the loading in the test was monotonic.

Material properties for specimens 3HN and CC-0 are provided in Table 2. Poisson's ratio for concrete is taken as 0.2.

Table 2 – Details of specimens 3HN and CC-0 with material properties for concrete and steel

Specimen	Dimensions			Concrete		Steel		
	D [mm]	t [mm]	L [mm]	f_c' [MPa]	E [GPa]	f_y [MPa]	E [GPa]	Poisson ration
3HN	150.0	3.20	450	28.7	-	287.4	200.0	0.300
CC-0	139.1	2.79	420	41.2	23.09	388.5	203.8	0.279

3. VALIDATION OF THE PROPOSED MODELS

Proposed models have been validated against test results and FE modelling results provided in the literature. Here the validation is presented for two circular specimens 3HN [13] and CC-0 [8] test results. Figures 4 and 5 demonstrate axial load–axial strain *(N-ε)* diagrams for the column specimens obtained in tests with the results of the proposed FE Models 1-3.

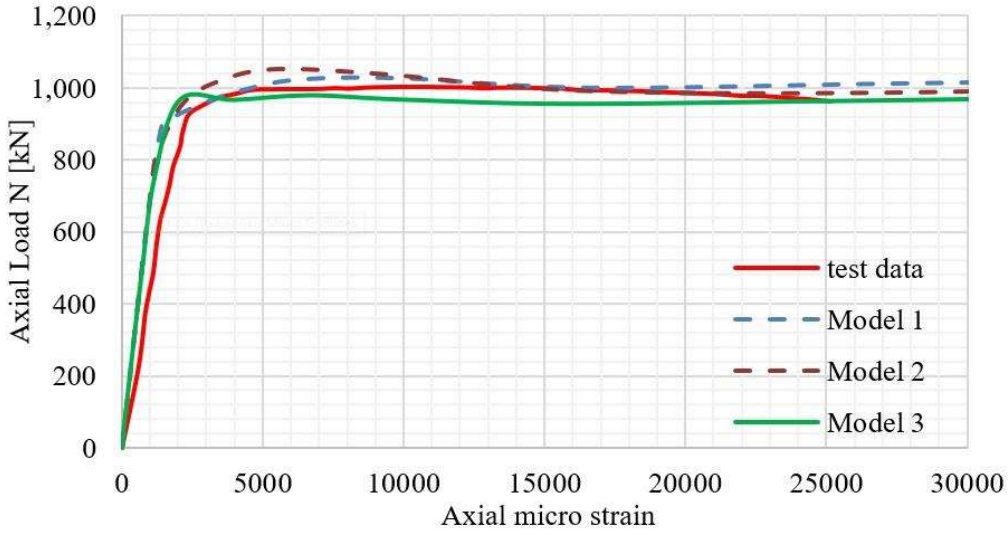

Figure 4 –N-ε diagram for specimen 3HN

As shown in Figure 4, there is generally good agreement between numerical and test results regarding the shape of the full-range *N-ε* diagram. Still, neither of the three models matches the test results during the initial elastic stage. As assumed, this probably occurred due to change in elastic modulus of concrete obtained from the tests [11]. Besides, Model 3 demonstrates a small peak in total strength and slightly underestimates the total strength. After reaching ultimate strength, all curves match the flattening part of the test curve.

Figure 5 shows the *N-ε* diagram for specimen CC-0. The results of all three models have satisfying accuracy.

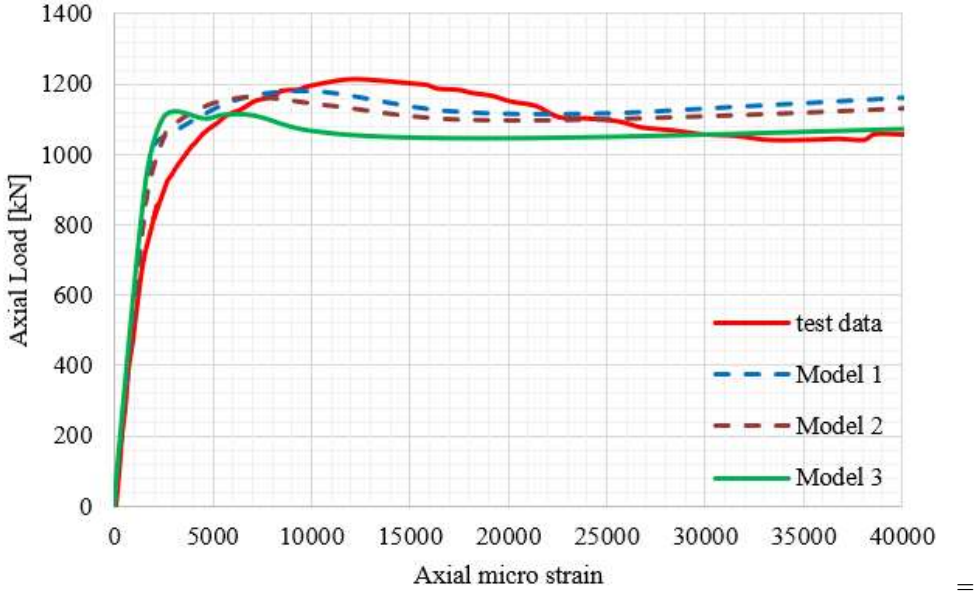

Figure 5 – N-ε diagram for specimen CC-0

Figure 6 shows the typical failure mode of the stub CFST column under axial load obtained in the analysis, presented for specimen 3HN.

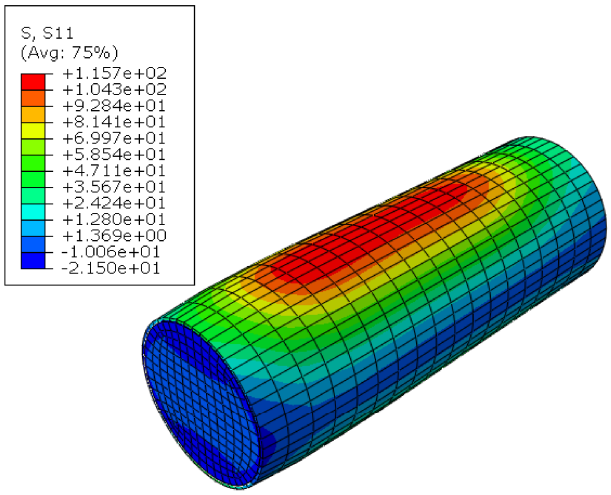

Figure 6 – Typical failure mode of stub circular specimen under axial load

The numerical ultimate strength values *Nu* from Figures 4 and 5 for Models 1-3 are compared to the test values $N_{u(test)}$ and well predicted, as presented in Table 3. Differences for both specimens remain within the range of 5%, except for Model 3 of the specimen CC-0, which equals 8,94%.

Table 3 – Summary of ultimate axial strength Nu results

	3HN		CC-0	
	N_u [kN]	$N_u/N_{u(test)}$ [%]	Nu [kN]	$N_u/N_{u(test)}$ [%]
test data	1001.17	100.00	1211.60	100.00
Model 1	1026.80	97.50	1178.42	102.82
Model 2	1052.66	95.11	1163.81	104.11
Model 3	980.35	102.12	1112.16	108.94
EC4	1174.76	85.22	1339.59	90.45

According to EC4, the ultimate plastic resistance to compression of a stub composite column $N_{u,EC4}$ is calculated from Eq. (2). For concrete-filled tubes of circular sections, it considers the decrease in steel strength by factor η_a and increase in strength of concrete caused by confinement factor η_c, Eq. (3-4). The buckling effective length was taken as 0.5 cooresponding to the fixed-ended boundary conditions in tests.

$$N_{u,EC4} = \eta_a A_a f_y + A_c f_c' \left(1 + \eta_c \frac{t}{d} \frac{f_y}{f_{c'}}\right) \quad (2)$$

$$\eta_a = 0.25(3 + 2\bar{\lambda}) \leq 1.0 \quad (3)$$

$$\eta_c = 4.9 - 18.5\bar{\lambda} + 17(\bar{\lambda})^2 \geq 0 \quad (4)$$

where:
A_a and A_c are cross-sectional areas of steel tube and concrete core respectively,
f_y is the nominal value of the yield strength of structural steel,
f_c' is characteristic compressive cylinder strength of concrete,
t is the wall thickness of the steel tube,
d is the external diameter of the column,
$\bar{\lambda}$ is the relative slenderness.

4. CONCLUSION

Numerical modelling in ABAQUS software offers powerfull capabilities for numerical modeling of nonlinear behavior of CFST columns. The presented 3D finite element models successfully simulate the behaviour of circular CFST stub columns under axial compression. The full range response of the columns through *N–ε* diagrams and failure modes has been validated against tests with satisfying accuracy. Models 1 and 2, based on previous recommendations, are confirmed to simulate the actual behaviour very well within 5% differences. On the other hand, EC2 proposes stress-strain relation for concrete in compression limited to 3.5‰ strain and no relation for concrete in tension. Even EC4 does not provide instructions regarding modelling of nonlinear behaviour of concrete inside the steel tube. Concrete material curve should include the

confinement strengthening especially beyond the current strain limit in the descending branch of the curve. Therefore, in the paper, a simple proposal was made to extend this curve to consider the effect of confinement. Model 3 showed good agreement with test results regarding the full-range N-ε diagram. The simplified EC4 section strength calculations are moderately conservative but accurate enough for practical applications.

ACKNOWLEDGEMENTS

The financial support of the Ministry of Education, Science and Technological Development, Republic of Serbia, through the project 200092, is acknowledged.

REFERENCES

[1] M. L. Radovanovic, J. Z. Nikolic, J. R. Radovanovic, and S. M. Kostic, Structural Behaviour of Axially Loaded Concrete-Filled Steel Tube Columns during the Top-Down Construction Method, Applied Sciences, vol. 12, no. 8, Apr. 2022, doi: 10.3390/app12083771.

[2] Y. F. Yang and L. H. Han, Concrete filled steel tube (CFST) columns subjected to concentrically partial compression, Thin-Walled Structures, vol. 50, no. 1, pp. 147–156, Jan. 2012, doi: 10.1016/J.TWS.2011.09.007.

[3] F. xing Ding, W. jun Wang, D. ren Lu, and X. mei Liu, Study on the behavior of concrete-filled square double-skin steel tubular stub columns under axial loading, Structures, vol. 23, pp. 665–676, Feb. 2020, doi: 10.1016/j.istruc.2019.12.008.

[4] Y. Gunawardena and F. Aslani, Finite element modelling of concrete-filled spiral-welded mild-steel tube short and long columns, Structures, vol. 30, pp. 1020–1041, Apr. 2021, doi: 10.1016/j.istruc.2021.01.074.

[5] Z. Bin Wang, Z. Tao, L. H. Han, B. Uy, D. Lam, and W. H. Kang, Strength, stiffness and ductility of concrete-filled steel columns under axial compression, Engineering Structures, vol. 135, pp. 209–221, Mar. 2017, doi: 10.1016/j.engStructures2016.12.049.

[6] N. F. Hany, E. G. Hantouche, and M. H. Harajli, Finite element modeling of FRP-confined concrete using modified concrete damaged plasticity, Engineering Structures, vol. 125, pp. 1–14, Oct. 2016, doi: 10.1016/j.engStructures2016.06.047.

[7] E. Ellobody, Nonlinear behaviour of eccentrically loaded FR concrete-filled stainless steel tubular columns, Journal of Constructional Steel Research, vol. 90, pp. 1–12, 2013, doi: 10.1016/j.jcsr.2013.07.018.

[8] V. W. Y. Tam, Z. Bin Wang, and Z. Tao, Behaviour of recycled aggregate concrete filled stainless steel stub columns, Materials and Structures, vol. 47, no. 1–2, pp. 293–310, Jan. 2014, doi: 10.1617/s11527-013-0061-1.

[9] Y. Tang, S. Fang, J. Chen, L. Ma, L. Li, and X. Wu, Axial compression behavior of recycled-aggregate-concrete-filled GFRP–steel composite tube columns, Engineering Structures, vol. 216, Aug. 2020, doi: 10.1016/j.engStructures2020.110676.

[10] W. H. Zhang, R. Wang, H. Zhao, D. Lam, and P. Chen, Axial-load response of CFST stub columns with external stainless steel and recycled aggregate concrete: Testing, mechanism analysis and design, Engineering Structures, vol. 256, Apr. 2022, doi: 10.1016/j.engStructures2022.113968.

[11] Z. Tao, Z. Bin Wang, and Q. Yu, Finite element modelling of concrete-filled steel stub columns under axial compression, Journal of Constructional Steel Research, vol. 89, pp. 121–131, 2013, doi: 10.1016/j.jcsr.2013.07.001.

[12] R. U. D. S. C. Providence, ABAQUS, User manual. Version 6.9. 2009.

[13] Y. M. M. Tomii, K. Yoshimura, Experimental studies on concrete filled steel tubular stub columns under concentric loading, in Proceedings of the International Colloquium on Stability of Structures under Static and Dynamic Loads, 1977, pp. 718–741.

[14] European committee for standardization, EN 1994-1-1: Eurocode 4: Design of composite steel and concrete structures-Part 1-1: General rules and rules for buildings, 2004.

[15] Deretić-Stojanović Biljana, Kostić Svetlana, and Stošić Saša, Analysis of composite steel and concrete columns, Building materials and structures, vol. 54, no. 1, pp. 62–79, 2011

[16] L. H. Han, G. H. Yao, and Z. Tao, Performance of concrete-filled thin-walled steel tubes under pure torsion, Thin-Walled Structures, vol. 45, no. 1, pp. 24–36, Jan. 2007, doi: 10.1016/j.tws.2007.01.008.

[17] European committee for standardization, prEN 1992-1-1: Design of concrete structures - Part 1-1: General rules - Rules for buildings, bridges and civil engineering structures, 2021.

[18] European committee for standardization, EN 1993-1-1: Eurocode 3: Design of steel structures - Part 1-1: General rules and rules for buildings, 2005.

[19] G. B. Hajjar JF, A cyclic nonlinear model for concrete-filled tubes formulation., Journal of Structural Engineering, ASCE, no. 123(6), pp. 736–44, 1997.

[20] J. M. Portolés, M. L. Romero, F. C. Filippou, and J. L. Bonet, Simulation and design recommendations of eccentrically loaded slender concrete-filled tubular columns, Engineering Structures, vol. 33, no. 5, pp. 1576–1593, May 2011, doi: 10.1016/j.engStructures2011.01.028.